Resistance to Strain Degradation in Preliminary UWMAK TF Coil Conductors for Fusion Reactors

S.O. Hong, P.F. Michaelson, I.N. Sviatoslavsky, and W.C. Young

November 1977

UWFDM-224

FUSION TECHNOLOGY INSTITUTE

UNIVERSITY OF WISCONSIN

MADISON WISCONSIN

Resistance to Strain Degradation in Preliminary UWMAK TF Coil Conductors for Fusion Reactors

S.O. Hong, P.F. Michaelson, I.N. Sviatoslavsky,
and W.C. Young

Fusion Technology Institute
University of Wisconsin
1500 Engineering Drive
Madison, WI 53706

http://fti.neep.wisc.edu

November 1977

UWFDM-224

Resistance to Strain Degradation in Preliminary UWMAK TF Coil Conductors for Fusion Reactors

S. O. Hong
P. F. Michaelson
I. N. Sviatoslavsky
W. C. Young

November 1977

UWFDM-224

Fusion Research Program
Nuclear Engineering Department
University of Wisconsin
Madison, Wisconsin 53706

Presented at the International Cryogenic Materials Conference, Boulder, Colorado, August 1977 and to be published in Advances in Cryogenic Engineering, Volume 24.

Resistance to Strain Degradation in Preliminary UWMAK TF Coil Conductors for Fusion Reactors

S. O. Hong, P. F. Michaelson, I. N. Sviatoslavsky and W. C. Young

University of Wisconsin
Madison, Wisconsin 53706

Introduction

The toroidal field (TF) magnets of the conceptual designs for tokamak fusion reactors performed at the University of Wisconsin[1] (UWMAK) consist of solid coils bolted together to form constant tension "D" shaped structures. Each coil consists of a forged or extruded helically grooved solid disk of stainless steel or aluminum alloy. The conductor (see Figure 1) is wrapped with fiberglass tape for electrical insulation and impregnated with epoxy and embedded in these grooves on both sides of the disk. After oven curing, the fiberglass on the exposed surface of the conductor is machined off for cooling in a pool of liquid helium. The coils are spaced apart with micarta spacers to allow free movement of the coolant throughout the structure.

For large magnets, the three major advantages of the embedded conductor structural disk design are: 1) the most efficient utilization of structural material for both radial and lateral loads, with the possibility of pre-stressing the structure during winding in order to put the conductor in compression; 2) minimizing conductor movement thus reducing heat generation due to friction; and 3) the capability of testing each disk in a cryostat under simulated operating conditions prior to assembling it into a completed magnet.

The primary objective of this experimental research has been to develop and test the embedded conductor design concept. In this paper the results of fatigue tests performed on a prototype model embedded conductor are reported, including the epoxy bond integrity, high voltage breakdown characteristic and the change in the resistance of the copper stabilizer due to the cyclic loading of the model at cryogenic temperature.

Cryogenic Epoxy Shear Stress Screening

A major question about the embedded conductor magnet design concerns the integrity of the bond between the conductor and the structural disk, in the environment of fusion reactor TF coils. A preliminary ring test and a quick survey of the data available on cryogenic shear strength of epoxies indicated that a screening test of bonding agents was needed in order to develop an optimum bonding technique for use during rigorous testing of the embedded conductor magnet concept.

Screening tests were made in liquid nitrogen using a loading mechanism, attached to an actuator and load cell, which can accommodate up to 12 specimens at a time. Each specimen consisted of a copper strip bonded with epoxy to a stainless steel strip. Servo control of the loading mechanism can be provided by sensing the overall load or the actuator displacement; however, strain gages on each of the stainless steel strips provided information on the load carried by each of the specimens. Bonding jigs were used to allow close control over joint thickness and to assure parallel alignment of the strips. The same stainless steel strips with the mounted strain gages were used over for additional tests.

Four strain gage rosettes were mounted on each stainless steel strip to form a bridge. Bridge output signal as a function of applied load was measured for each bridge at 300 K and for three bridges at 300 K and 77 K to calibrate the stainless steel strips as load cells. Each stainless steel strip was then bonded to a copper strip with a chosen adhesive. Data on shear stress at fracture of various bonding agents were obtained by cooling the complete specimen (stainless steel-adhesive-copper) in liquid nitrogen and increasing the strain in progressive steps, with the strain gage output recorded for each bridge at each load step. The load on a bond during the load step just prior to fracture divided by the bonding surface area is the reported shear stress at fracture. Preliminary results are listed in Table 1 for unfilled and unreinforced epoxies. Because the epoxy shear load is non-uniform in lap tests,[2] each reported value is the geometrical average of the shear stress in the bonded region, and thus is lower than the peak shear stress existing before fracture. When the bond lap length in the direction of tension (L) is reduced then the average shear stress increases to appraoch the peak shear stress. This means that reported values for shear stress at fracture will depend upon L, and explains why our results (measured with L = 0.63 cm) are roughly four times higher than those of Froelich and Fitzpatrick[3] (measured with L $\simeq$ 2.54 cm). The highest shear strengths obtained were 70 MPa (10,100 psi) for Crest 7410 and 65 MPa (9,500 psi) for Crest 391. On the basis of these results, it was decided to use Crest 391 on the top conductor and Crest 7410 on the bottom conductor in the ring test. Subsequent experiments in preparation for electrical breakdown tests indicated that Crest 7410 has a tendency to crack from thermal shock at cryogenic temperature which may be due to its relatively high modulus of elasticity.

Table 1

Maximum Shear Strength Measured at 77 K*

Adhesive	Shear Strength (MPa)	Shear Strength (psi)
CREST 7410	70.	(10,100)
CREST 391	65.	(9,500)
FM-123-2	53.	(7,700)
3M SCOTCHWELD 2214	39.	(5,700)
FM-73-M	39.	(5,600)
SHELL EPON 828	38.	(5,500)
CREST 3170	37.	(5,400)
CHEMLOK 304	28.	(4,100)
HT-424	28.	(4,000)
3M SCOTCHWELD 2216	26.	(3,700)
CREST 7344	24.	(3,500)
METLBOND 1113 (NARMCO)	18.	(2,600)
VERSILOK B-2415-45	14.	(2,000)

*For lap shear strength between copper and stainless steel strips

Ring Test Experimental Procedure

To simulate the radial cyclic magnetic loading in a fusion reactor TF coil a novel apparatus was designed and constructed which is capable of applying large uniform radial loads to a ring cyclically at cryogenic temperatures. The unique feature of this apparatus is the double split cone set shown in Figure 2. A compressive force applied vertically between the two cone apexes results in a radial force directed outward from each point on the cone edge circumference. The stainless steel ring with the embedded conductors fits on the outer circumferential edge of the split cones. It has an outer radius of 22 cm, an inner radius of 20 cm and is 3 cm thick. It has one single turn 1.06 x 1.06 cm groove machined in its top surface and one in its bottom surface with the conductors embedded in them. A force of 1.4×10^5 N, applied to the test cones by a hydraulic actuator, produces 0.2% strain at the outer perimeter of the stainless-steel ring.

In preparing for the test, the 1 cm x 1 cm OFHC copper conductor was rolled and cut to form two rings made to fit into the grooves of the stainless steel ring. Both the copper rings and the grooves were sandblasted and thoroughly cleaned and degreased. The copper conductors were wrapped with B-cured fiberglass tape, impregnated with the chosen epoxy and carefully fitted into the grooves of the test ring. After oven curing, the fiberglass epoxy on the exposed surface was machined off. The conductors were drilled and tapped for the current and voltage leads used to measure electrical resistance. Stainless steel pins, insulated with a thin layer of G-10, were inserted as shown in Figure 3 to reduce stress effects

close to the ends of the conductors. This provision simulates the boundary conditions of the conductors in a TF coil, where the conductor continues to spiral into adjacent grooves rather than terminating as in the test ring. Four pairs of strain gage rosettes were mounted around the outer perimeter of the test ring at mid-thickness for the control of the closed-loop feedback system driving the MTS hydraulic load actuator. Eleven strain gages were mounted on each side of the test ring, four on the copper conductor, six on the stainless steel and one on the epoxy across the end joint of the copper conductor as shown in Figure 3.

With leads wired properly to the gages and current and voltage terminals, the test ring was mounted on the loading cones. After all the instruments were properly assembled, the test ring and loading cones were attached to the actuator, sealed into the helium dewar, precooled with liquid nitrogen, and immersed in liquid helium.

The hydraulic actuator was driven by a function generator to automatically produce pure tension stress cycles in the test ring, each with a period of 20 seconds. After every 100 cycles the actuator was controlled with manual input for one cycle to allow pauses at intermediate load steps. At each such step the strain gages were scanned by a 30 channel Vishay/Ellis data recording system and the copper resistance was measured. The high voltage breakdown characteristic was measured after 1000 fatigue cycles had been completed.

Ring Test Experimental Results

The results obtained from the strain gages during fatigue cycling of the test ring are plotted in Figure 4. These data are for the conductor in the top half of the ring. We interpret these data to mean that the bond did not fail. (Unfortunately, the readings of the strain gages on the bottom conductor, which was instrumented exactly as the top, had a noise component large enough to obscure any meaningful data. Efforts to track down and correct this faulty condition were unsuccessful).

The rise in the strain at all the gages during the first 100 cycles is not completely understood, but was not due to a change in the loading mechanism. This was verified by measurements on our load cell. Possible explanations are "low cycle cryogenic fatigue creep" of the steel and/or small degradation of strain gages.

The strains indicated by gages 3 and 5 on the conductor are lower than the corresponding gages 4 and 6 on the steel. It must be understood that the steel pins were not forced into the ring with an interference fit and thus some relative motion between the conductor and the steel near the joint was allowed, accompanied by elastic deformation of the epoxy and a reduced strain level in the copper. This effect is not observed at gage 1, far from the copper joint, because enough load is picked up by the copper at gage 1 to give a reading close to those of the adjacent gages (0 and 2) on the steel. The progressive lowering of the strain at gage 3 may be due to plastic deformation of the insulation on the steel pins with repeated cycling. The relative order of strain level in gages 0, 1 and 2 is consistent with thick walled pressure vessel theory for vessels with internal pressure. The slight differences in the strains at gages 2, 4 and 6 are probably due to small variations in the applied radial load because of the imperfections in the conical loading mechanism.

In order to verify that the epoxy bonds had not failed during the 1000 fatigue cycles (a conclusion which is suggested but not confirmed by the data of Figure 4), the steel pins were removed and the test ring loaded once more, this time in liquid nitrogen, to a 0.2% strain level at the ring's outer perimeter (see Figure 5). Gages 0, 1 and 2 track each other very closely indicating that the Crest 391 epoxy bond at their location was intact.

Although the strain level at gage 3, close to the copper joint, lagged behind the strain at gage 4, its steady increase with increasing load indicates that the epoxy bond was intact here also. The lower strain level in gage 3 is due to the elastic deformation of the epoxy near the joint, which allows the copper to be strained less than the steel in that region. Note that the strain levels of gages 0, 1, 2, and 4 are lower than those measured between cycle 100 and 1000 shown in Figure 4, and are more like those of cycle 1, because a one day anneal at room temperature has removed the "low cycle cryogenic fatigue creep" and/or strain gage degradation.

Although we do not report the noisy data from the bottom gages of the test ring, there was some indication that the Crest 7410 epoxy bond failed during loading without the steel pins, and may also have failed somewhat during the preceeding fatigue cycling with the pins in place. The noise in the data was <u>not</u> caused by a failed epoxy bond.

The degradation of resistance of the copper conductor, shown in Figure 6, is very small (only a factor of 1.6) and tends to reach an asymptotic limit by cycle number 1000. Each resistance measurement was made at 4.2 K at zero hydraulic actuator load using a 50. ampere current. Before the

first cycle the residual resistance ratio (RRR = $R_{300\ K}/R_{4.2\ K}$) of the copper was 152. Fisher, Kim and Turner[4] found a similar degradation using samples of copper that were not bonded to a steel supporting structure, but which were cycled through tension - compression modes in an attempt to simulate the stress cycles expected for copper taken past its yield point while bonded into a non-yielding steel structure subjected to pure tension cycles.

Voltage breakdown across the 0.8 mm wide epoxy region between the stainless steel and the copper occurred at 2500 volts (see Figure 7) when measured in liquid helium after 1000 cryogenic fatigue cycles to 0.2% peak strain in the test ring outer perimeter. Above the breakdown voltage the current remained small. Repeated measurements gave identical results so the current path is not burned or degraded by the breakdown. Solder flux, small pieces or chips of metal, machine oil and other contaminants possibly present on or inside the epoxy may have reduced the breakdown voltage from a potentially higher value. As found in a related study,[5] Crest 391 epoxy on B-cured fiberglass tape in liquid helium has a breakdown voltage of 31. kV across a 0.25 mm thick sample in the non-uniform electric field near a sharply pointed voltage contact.

The double split cone loading mechanism worked well but the cone must be designed to match the circumferential stiffness at the test specimen. To minimize the required axial load and the cross sections of the actuator rods in order to reduce the heat load into the dewar one must design the cones to operate near the snap-through instability typical of Belleville springs. Details of the cone design will be reported elsewhere.

Conclusions

The integrity of the epoxy bond in embedded conductor magnets has been successfully demonstrated in an engineering prototype model to the stress and cycle number limits of proposed UWMAK reactors. The resistance change of the embedded conductor is small after fatigue cycling. The breakdown voltage across the epoxy bond in the prototype model is within a factor of two of the value (~ 5000 volts) projected in UWMAK design studies, and may possibly be increased in future magnets or models by using more careful and cleaner fabrication procedures, a larger epoxy bond gap width, or adding insulation on the structural steel adjacent to the conductor. Moreover, the breakdown value used in the UWMAK designs can be decreased if a longer time is assumed for discharging the magnet under a fault condition.

Acknowledgements

We would like to acknowledge the help and encouragement of Professor R. W. Boom and the aid of Dr. T. Richards and Mr. J. Dreger. The assistance of W. Craddock, J. Dobogai, J. Egan, J. Vallem, and R. Watson, all students at the U.W., is also appreciated. The authors acknowledge the Division of Magnetic Fusion Energy of ERDA for support of this work, and Phelps-Dodge Co. of Bayway, New Jersey for supplying the copper conductor.

References

1. W. C. Young and R. W. Boom, Proc. Fourth Int. Conf. on Magnet Technology, CONF-720908, Brookhaven, p. 244 (1972).

2. J. A. Graham, Machine Design, October 7, Volume 48, p. 118 (1976).

3. K. J. Froelich and C. M. Fitzpatrick, Lap Shear Strength of Selected Adhesives (Epoxy, Varnish, B-Stage Glass Cloth) in Liquid Nitrogen and at Room Temperature, Oak Ridge National Laboratory/Technical Memo 5658 (1976).

4. E. S. Fisher, S. H. Kim, and A. P. L. Turner, Proc. Conf. Int. Cryogenic Engineering, Grenoble, France (1976).

5. P. Hwang, U. of Wisconsin-Madison, private communication.

Figure Captions

Figure 1 Disk cross-section of UWMAK-II toroidal field magnets.

Figure 2 Stainless steel test ring with embedded copper conductors installed on double split cone set.

Figure 3 Test ring component layout, top side.

Figure 4 Bond integrity of test ring at 0.2% peak strain at outer perimeter at 4.2 K. Cycles are pure tension with 20. second period.

Figure 5 Bond integrity of test ring after 1000 fatigue cycles to 0.2% peak strain at outer perimeter at 4.2 K. measured at 77 K with steel pins removed from joint area.

Figure 6 Degradation of copper stabilizer resistance during fatigue cycling to 0.28% peak strain in the copper at 4.2 K.

Figure 7 Voltage breakdown characteristic of test ring in liquid helium after 1000 fatigue cycles to 0.2% peak strain at outer perimeter at 4.2 K. Triangles refer to large, abrupt voltage steps; circles refer to small, gradual voltage steps.

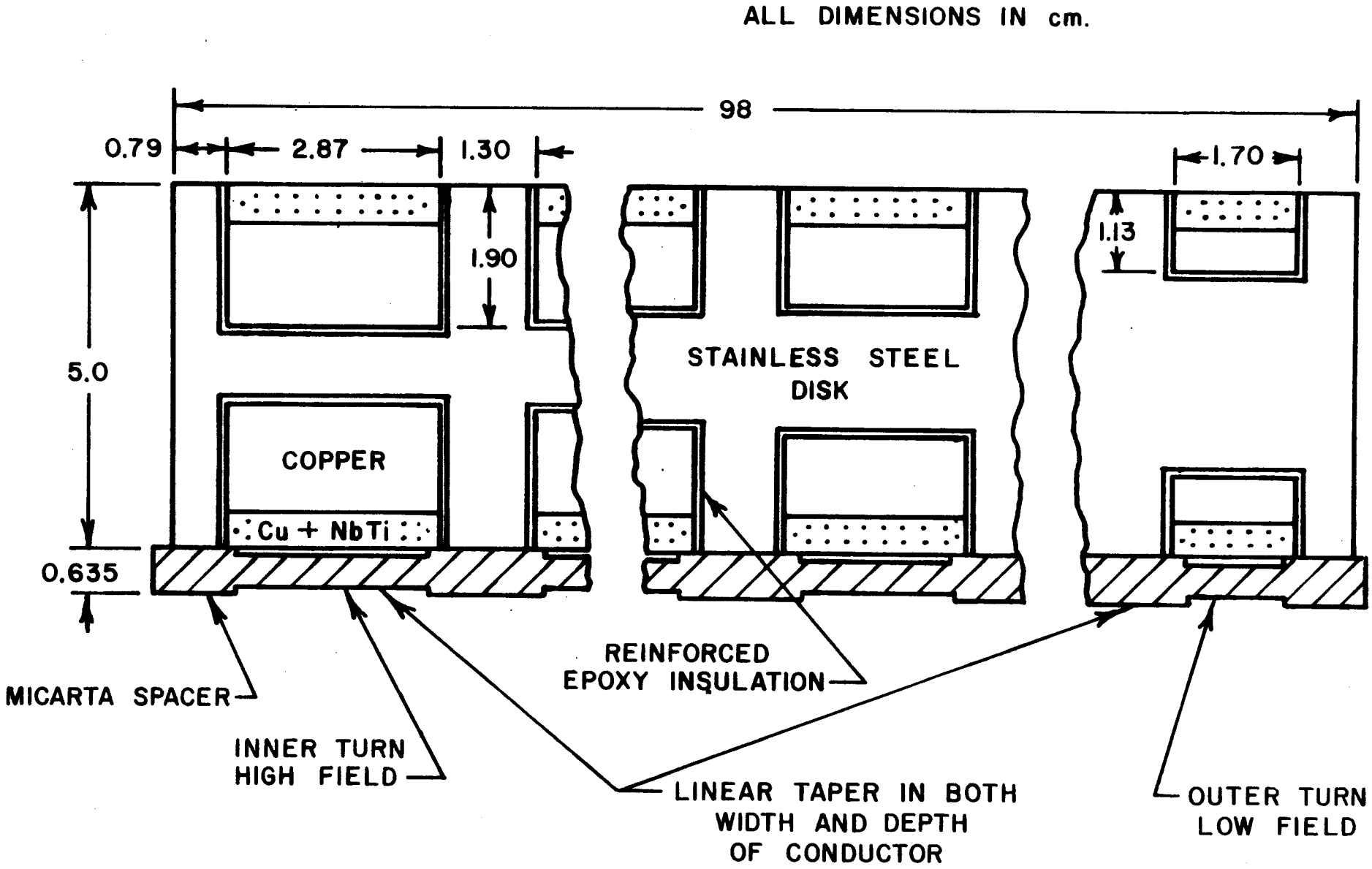
ALL DIMENSIONS IN cm.
98
0.79
2.87
1.30
1.70
1.90
1.13
5.0
0.635
COPPER
Cu + NbTi
STAINLESS STEEL
DISK
MICARTA SPACER
INNER TURN
HIGH FIELD
REINFORCED
EPOXY INSULATION
LINEAR TAPER IN BOTH
WIDTH AND DEPTH
OF CONDUCTOR
OUTER TURN
LOW FIELD

Figure 1

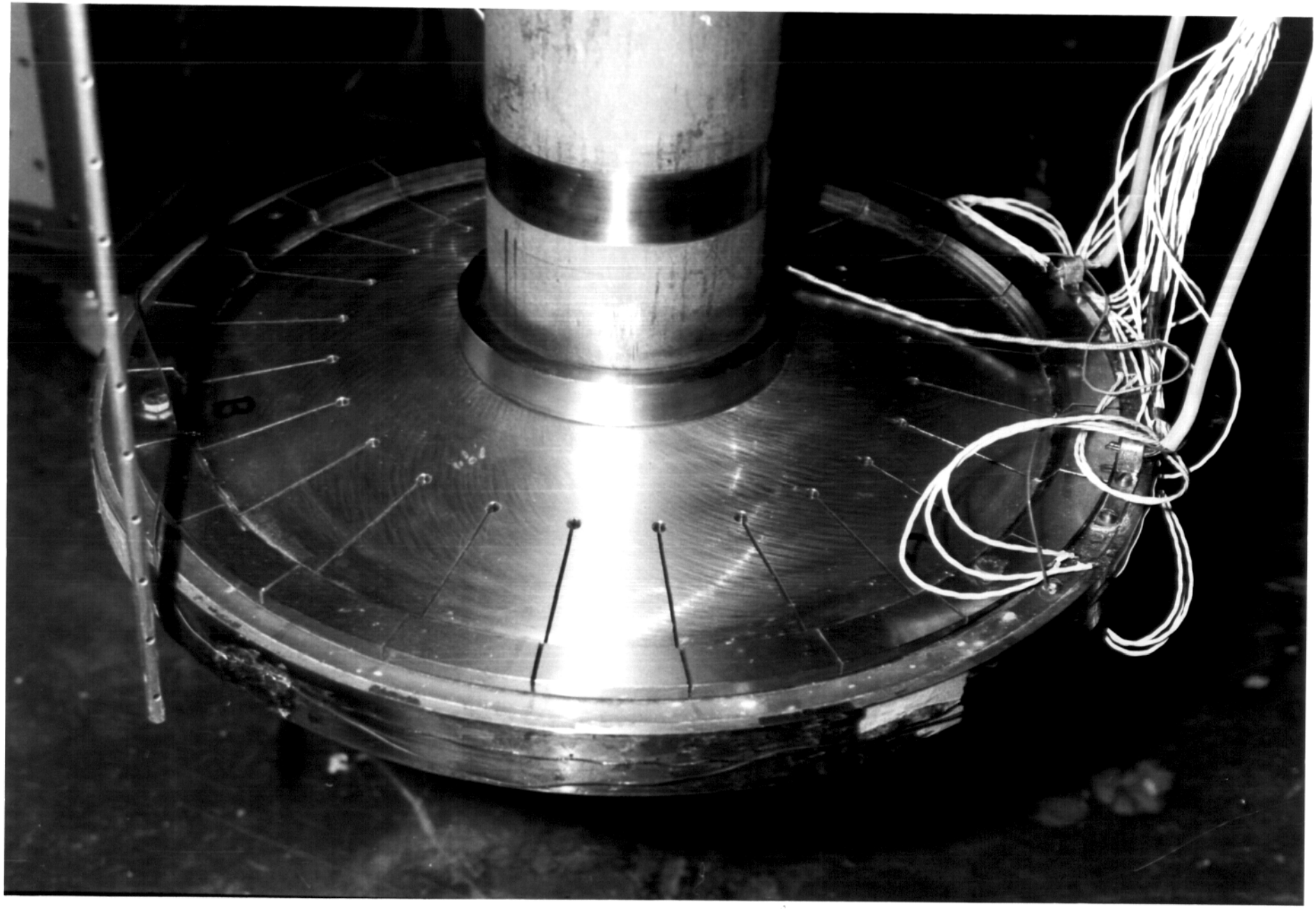

Figure 2

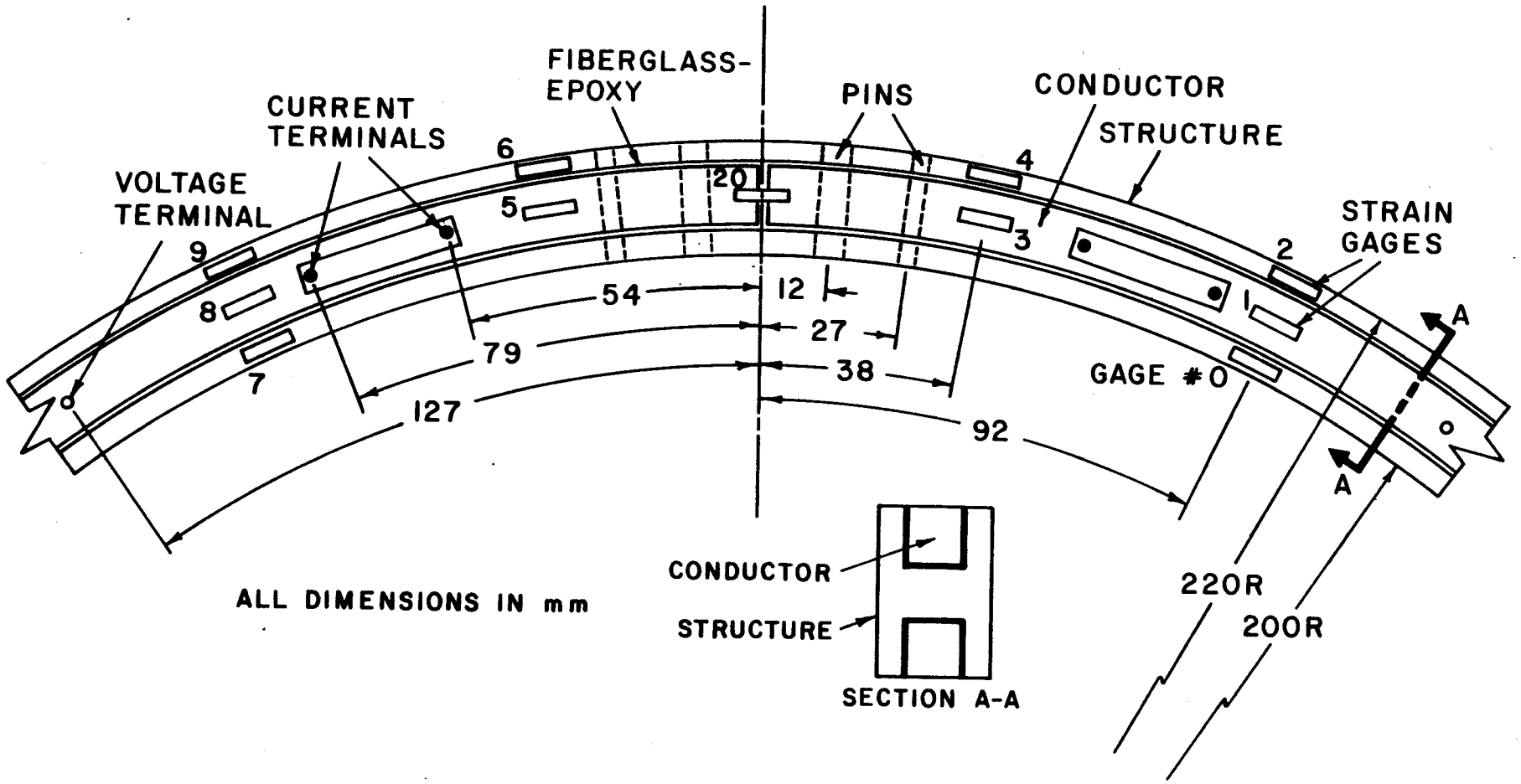
FIBERGLASS-
EPOXY
PINS
CONDUCTOR
STRUCTURE
CURRENT
TERMINALS
VOLTAGE
TERMINAL
STRAIN
GAGES
9
8
7
6
5
4
3
2
1
20
54
12
27
79
38
127
92
GAGE #0
A
A
ALL DIMENSIONS IN mm
CONDUCTOR
STRUCTURE
SECTION A-A
220R
200R

Figure 3

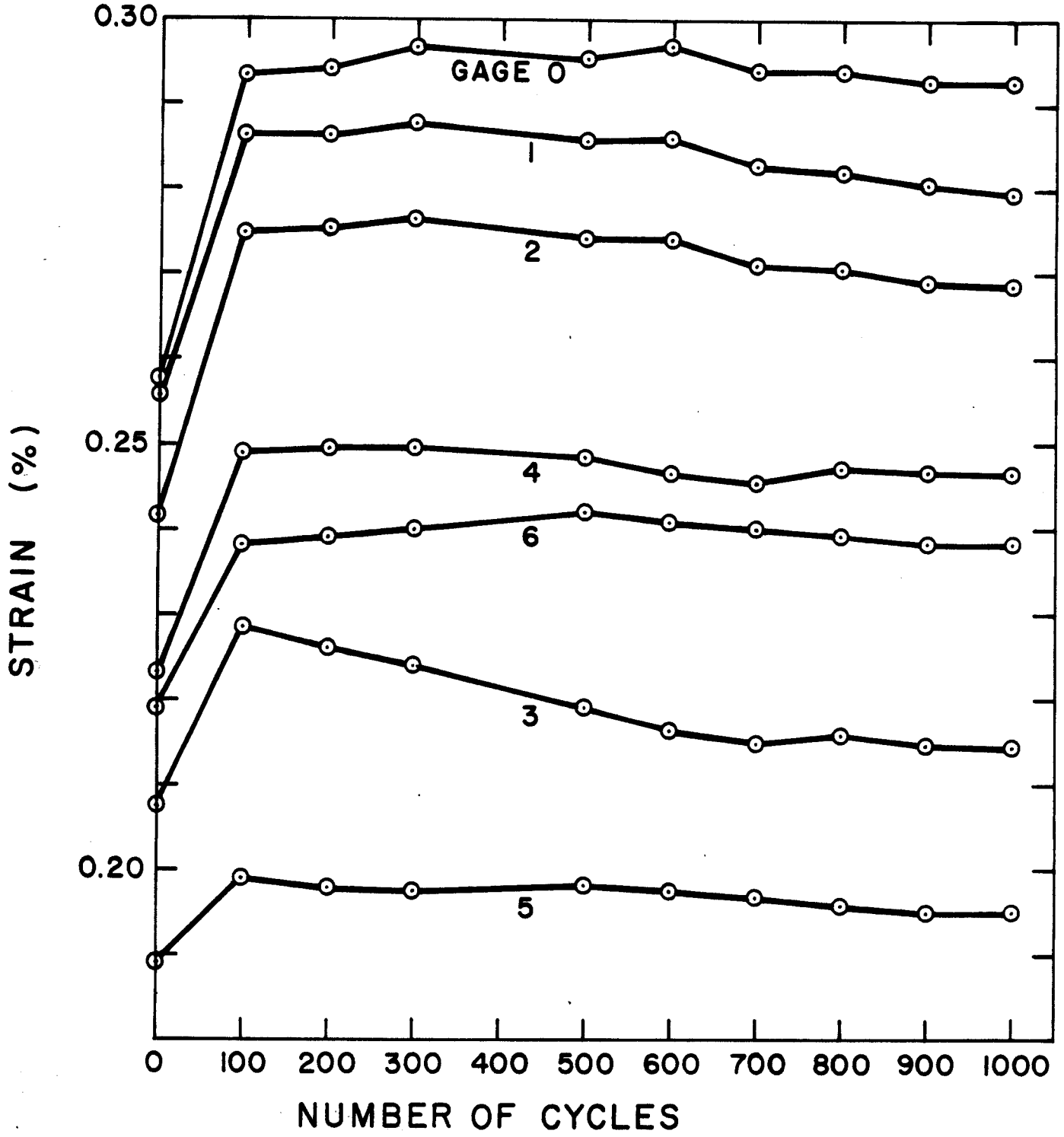
0.30
0.25
0.20
STRAIN (%)
GAGE 0
1
2
4
6
3
5
0
100
200
300
400
500
600
700
800
900
1000
NUMBER OF CYCLES

Figure 4

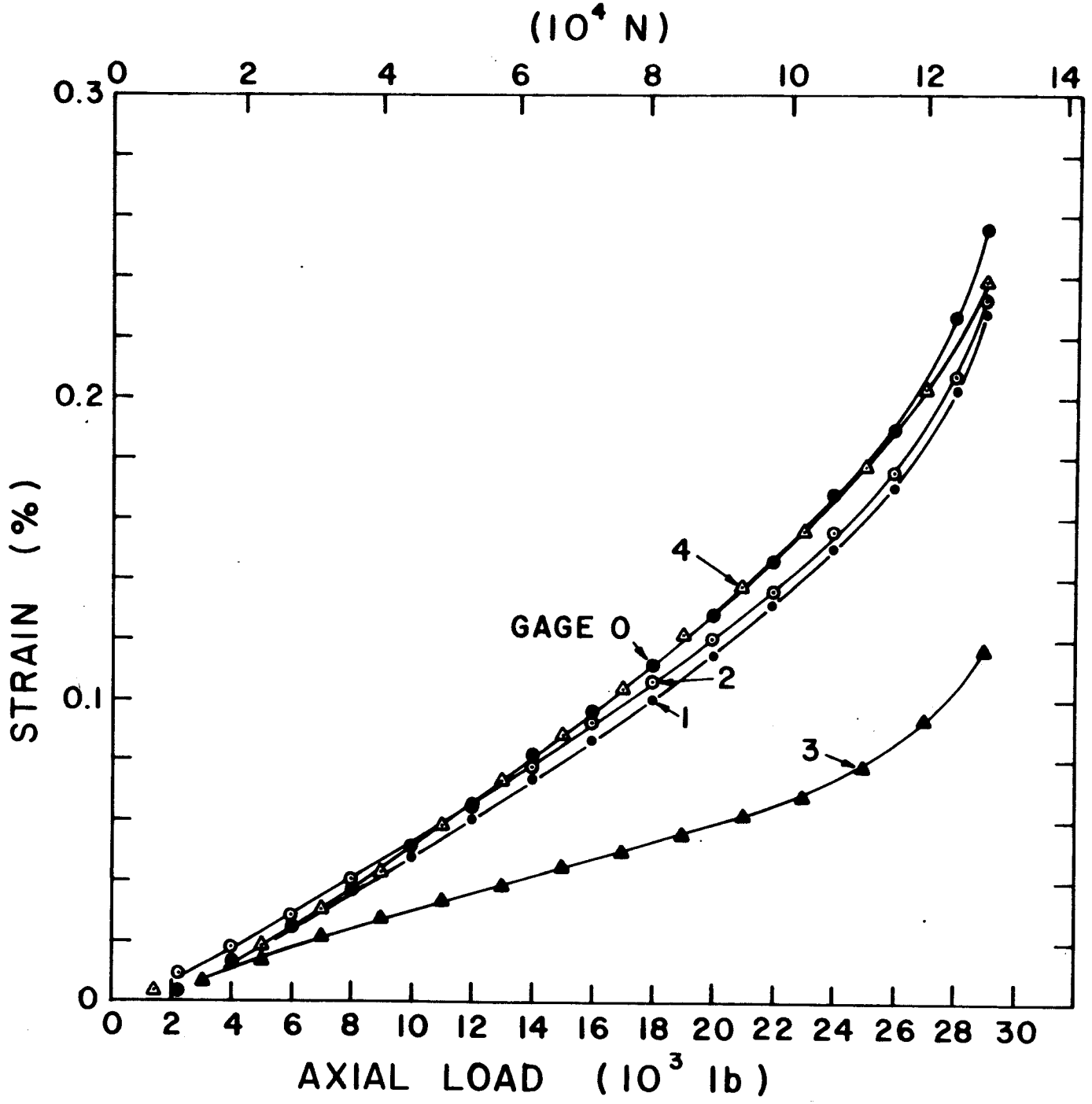
(10⁴ N)
0
2
4
6
8
10
12
14
0.3
0.2
0.1
0
STRAIN (%)
GAGE 0
1
2
3
4
0
2
4
6
8
10
12
14
16
18
20
22
24
26
28
30
AXIAL LOAD (10³ lb)

Figure 5

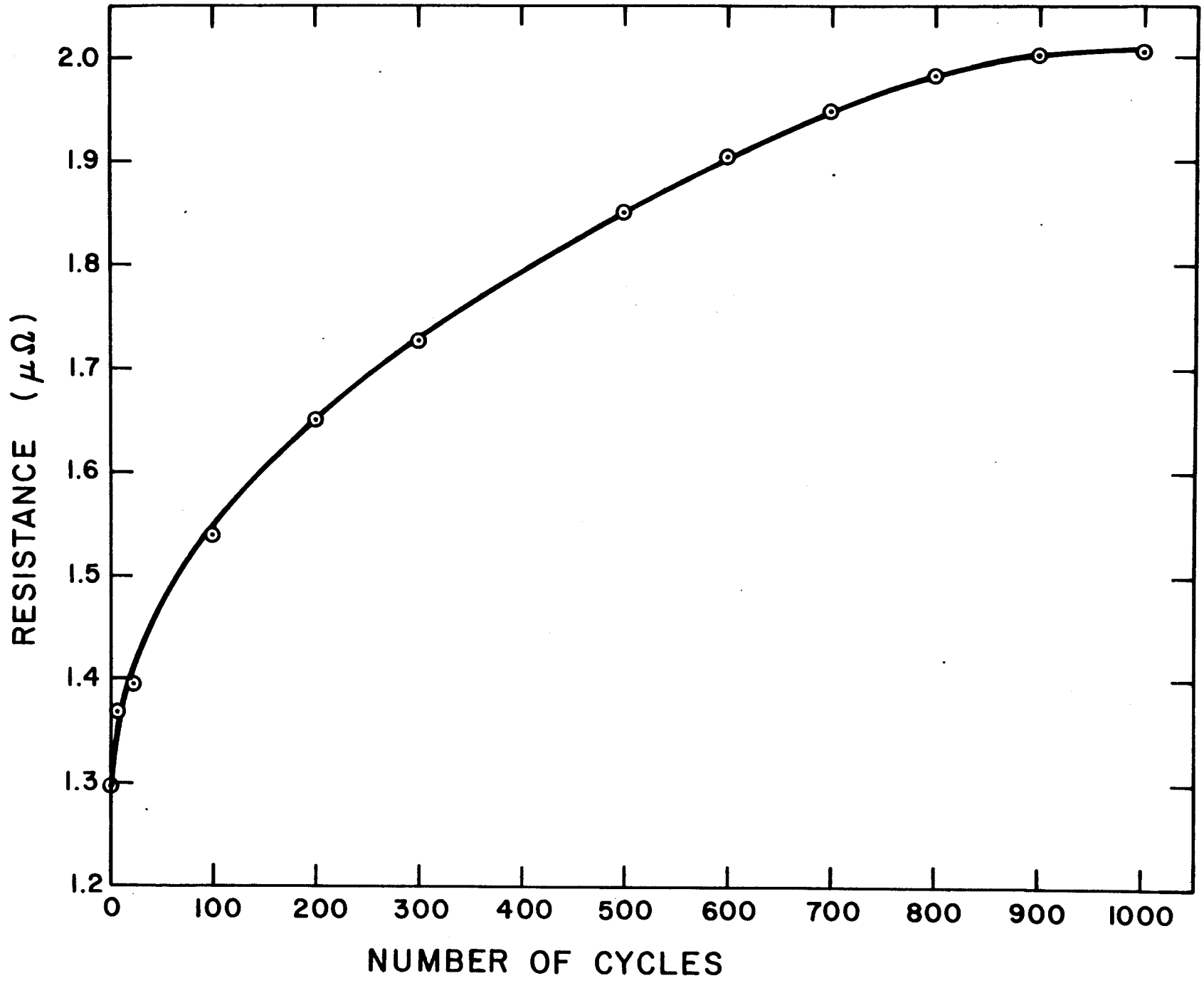
RESISTANCE (μΩ)
2.0
1.9
1.8
1.7
1.6
1.5
1.4
1.3
1.2
0
100
200
300
400
500
600
700
800
900
1000
NUMBER OF CYCLES

Figure 6

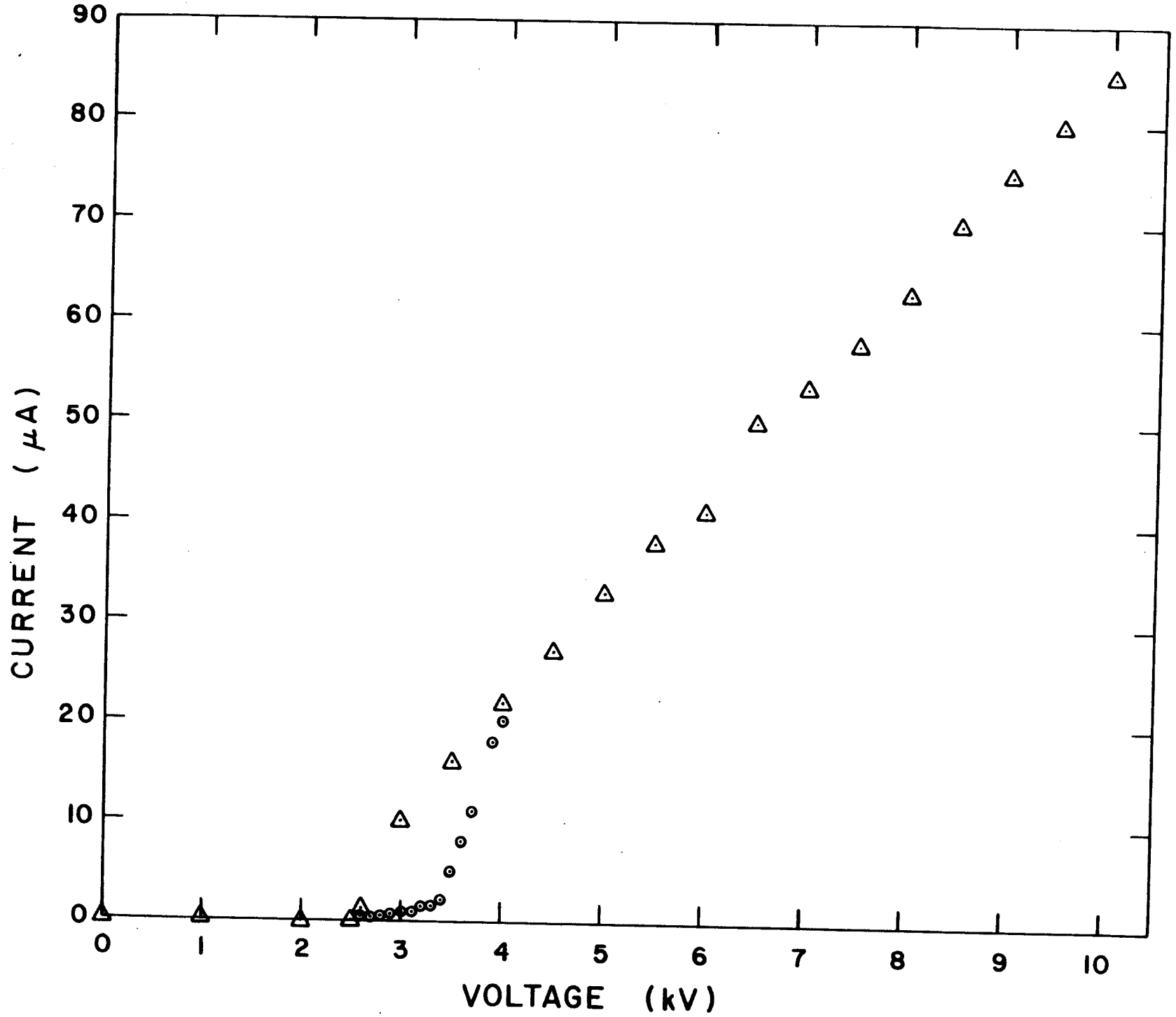

Figure 7